Electronic Supplementary Material (ESI) for Analyst.

Supplementary Material

Spatially-extended 3D Magnetic DNA Nanodevice-Based Split-Type photoelectrochemical Strategy for Sensitive and Reliable MiRNA Detection in Cancer Cells

Hui Yuan,[a] Jiuming Sun,[a] Qi Zhang,[a] Mingyue Chu,[a] Guiguang Cheng,[b] Xia Li,[*a] Qingwang Xue[*a]

[a]*School of Chemistry and Chemical Engineering, Liaocheng University, Liaocheng 252059, China*

[b]*Faculty of Agriculture and Food, Kunming University of Science and Technology, Kunming, China*

Correspondence: lixia@lcu.edu.cn (X. L.); xueqingwang1983@163.com (Q-W. X)

Table of Contents

Experimental section

Chemicals

Methylene blue (MB), Deoxynucleotide triphosphates (dNTPs) and all the HPLC-purified oligonucleotide sequences were obtained from Sangon Biotech Co., Ltd. (Shanghai, China). DNA oligonucleotide sequences were shown in **Table S1**. T4 DNA ligase, phi 29 DNA polymerase, rNTP Mix and RNase inhibitor were purchased from New England Biolabs, Ltd (Beijing, China). Streptavidin-magnetic nanobeads (streptavidin-MBs, the mean diameter is 300 nm) were purchased from Biomag Biotechnology Co., Ltd (Wuxi, China). All other reagents were of analytical grade. All aqueous solutions were prepared using ultra-pure water (≥18 MΩ cm^{-1}) and treated with DEPC.

Apparatus

Agarose gel electrophoresis analysis was performed on an electrophoresis analyzer and gel imaging was accomplished on a Molecular Imager® GelDoc™ XR+ imaging system (Bio-Rad, USA). All photoelectrochemical tests were measured on ZAHNER-PP21 (Zana, Germany). The UV-vis absorption spectra were collected on a UH-4150 spectrophotometer (Hitachi, Japan). AFM were collected on Bruker Multimode 8 (USA). Isothermal titration calorimetry (ITC) experiments were carried out using a MicroCal ITC200 titration calorimeter (GE Healthcare, USA).

Preparation and of space-expanded 3D magnetic DNA nanodevice

The first stage of space-expanded 3D magnetic DNA nanodevice involves the target recognition and RCA amplification reaction process, which was performed in a homogeneous solution as follows: target miR-21 and padlock probe were mixed in 1×T4 DNA ligase buffer (40 mM Tris-HCl, 10 mM $MgCl_2$, 10 mM DTT, 0.5 mM ATP, pH 7.80). The mixture was heated to 90 °C for 5 min and then slowly cooled to room temperature, yielding circular DNA with a nick. Subsequently, the nicked

circular DNA was connected by incubation with T4 DNA ligase in 10×T4 DNA ligase buffer overnight ligation reaction followed by 65 °C for 10 min. Second, the RCA reaction occurred at 37 °C for 2 h with the addition of 10× phi 29 DNA polymerase buffer, phi 29 DNA polymerase and dNTP followed by 65 °C for 10 min. The mixture for the resulting DNA strands and three primers (biotin-P1, P2 and P3) were incubated in TAE/Mg^{2+} buffer (20 mM Tris, 10 mM acetic acid, 1 mM EDTA and 6.25 mM magnesium acetate, pH 7.60) solution, which was heated to 90 °C for 5 min and then slowly cooled to room temperature, folding into predetermined high-order DNA scaffolds. Finally, streptavidin-modified MB was added to the above solution, and high-order DNA scaffolds were anchored to magnetic particles through avidin-biotin to form 3D magnetic DNA nanodevices.

Construction of Split-type "turn-off" PEC biosensor

In order to obtain the negatively charged FTO electrode surface for PEC measurement, the processing involved was shown in Supplementary Material (part I). The as-mentioned magnetic DNA nanodevices were transferred the into 30 μL (1mg/ml) MB solution (containing 0.1 M Ascorbic Acid (AA) and 0.2 M Na_2SO_4, pH 7.80) and was incubated at 37 ° C for 2 h. The visible light source (λ=629 nm) is used to 15 s (**Fig.S2**). After magnetically separated of the bound MB with the as-designed magnetic DNA nanodevice, the photocurrent signal for the rest of the MB solution was measured towards bare FTO electrode. The bare FTO electrodes with surface area 2.5 cm × 3 cm were ultrasonically cleaned for 1 h in 1 M NaOH, water/ethanol (1:1, V/V), acetone and ultra-pure water, followed by blown dry with nitrogen gas, respectively. Upon visible light illumination (**Fig. S2**), the MB can transform to leuco-MB, and the subsequent current generation occurs in the presence of strong reducing agents AA as illustrated below.

$$MB \xrightarrow{hv} MB^*$$

$$MB^* + AA \rightarrow \text{leuco-MB} + \text{oxidezed AA}$$

$$\text{leuco-MB} \rightarrow \text{MB} + e^-$$

Agarose gel electrophoresis analysis

For agarose gel electrophoresis analysis, the RCA amplification products and the resulting high-order folded DNA nanostructure were run on 2% agarose gel electrophoresis in 1×TAE buffer for 45 min with a constant voltage of 90 V at 0 ° C, followed by the EB staining and visualization in gel imaging system (Molecular Imager® GelDoc™ XR+)

Isothermal titration calorimetry

All ITC experiments were conducted using MicroCal ITC200 titration calorimeter using protocols developed in our laboratory. For all ITC measurements, the reference power and stirring speed were set at 5 μcal·s^{-1} and 750 rpm, respectively. The calorimetric experiments were run at 310.15 K. The sample cell was filled with 4 μM high-order DNA scaffolds solution. In each titration experiment, 20 injections of 2 μL 500 μM MB solution (with an initial injection of 0.4 μL) were titrated into the sample cell. All the data were analyzed and plotted using Origin 7.0 software provided by the ITC200 calorimeter.

Cell lines and cell culture

A human cervical cancer cell line (HeLa), a human lung cancer cell line (A549) and a hepatocellular carcinoma cell line (HepG2) were cultured in cell culture medium mixed with 10% FBS and 1% penicillin streptomycin. All cells were first incubated at 37 °C in a humidified atmosphere of 5% CO_2.

Table S1. Sequences of oligonucleotides used in this study

Name	Sequence (5'-3')
Padlock	P-CTG ATA AGC TAT AAG ATG AAG ATA GCG CAC AAT GGT CGG ATT CTC AAC TCG TAT TCT CAA CTC GTA TTC TCA ACT CGT TCA ACA TCA GT
Short chain 1	Biotin-CCC TGA CTC ACA ATG GTC GGA TTC CGT CTC TG
Short chain 2	CAG CCC TGT AAG ATG AAG ATA GCG TCT ATG CC
Short chain 3	TCT CAA CTT CAA CTC GTA TTC TCA ACT CGT AT
miR-21	UAG CUU AUC AGA CUG AUG UUG A
Let-7a	UGA GGU AGU AGG UUG UAU AGU U
miR-141	UAA CAC UGU CUG GUA AAG AUG G
miR-155	UUA AUG CUA AUC GUG AUA GGG GU

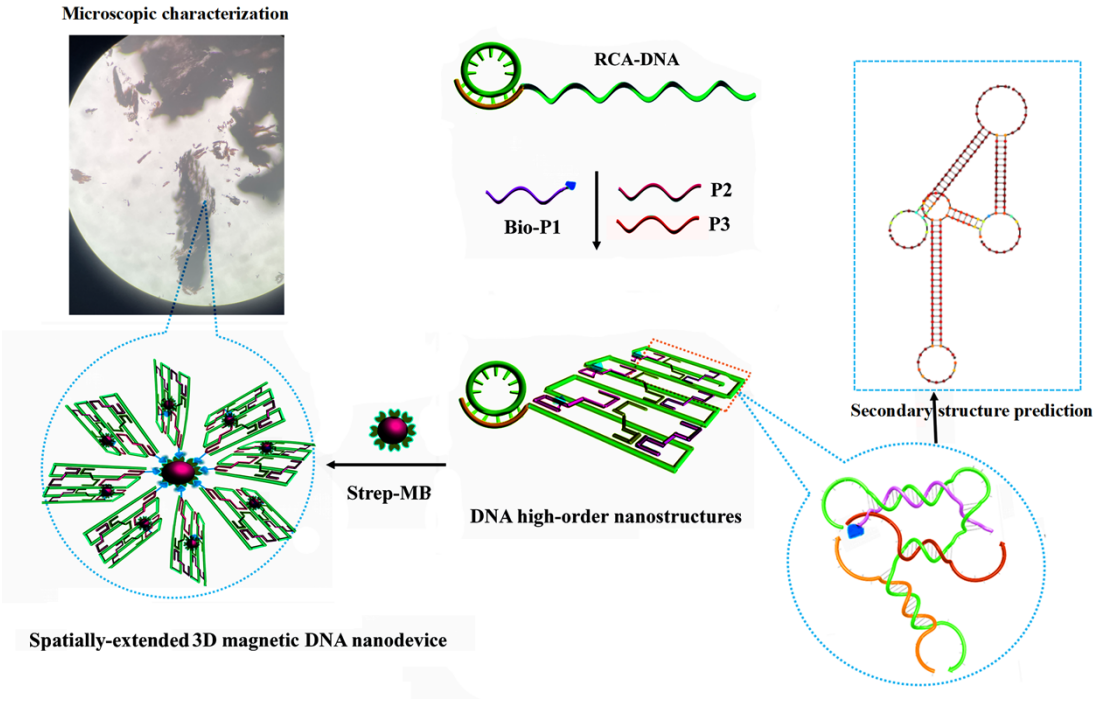

Fig. S1. The second structure of high folded DNA scaffolds unit and the microscopic characterization of the 3D magnetic DNA nanodevices

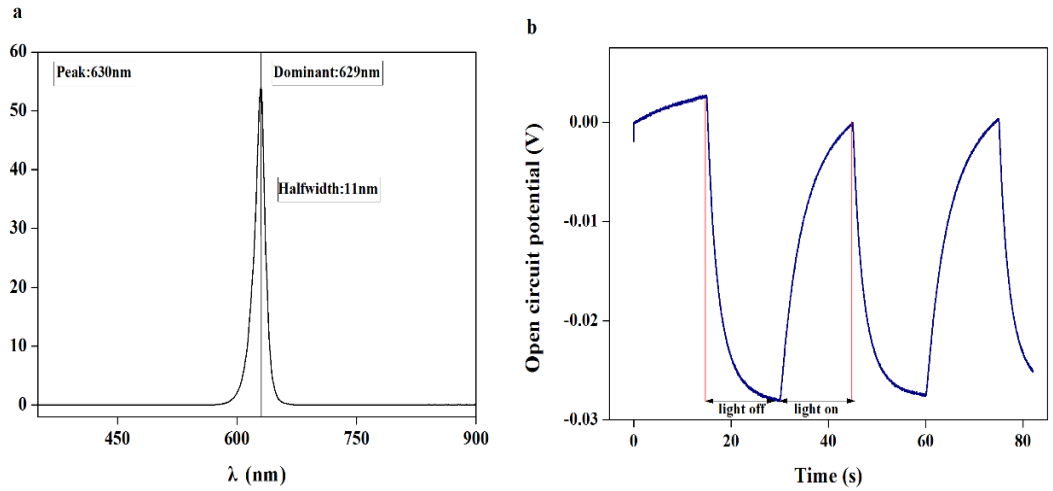

Fig. S2. The selection of light source wavelength (a) and switching time interval (b)

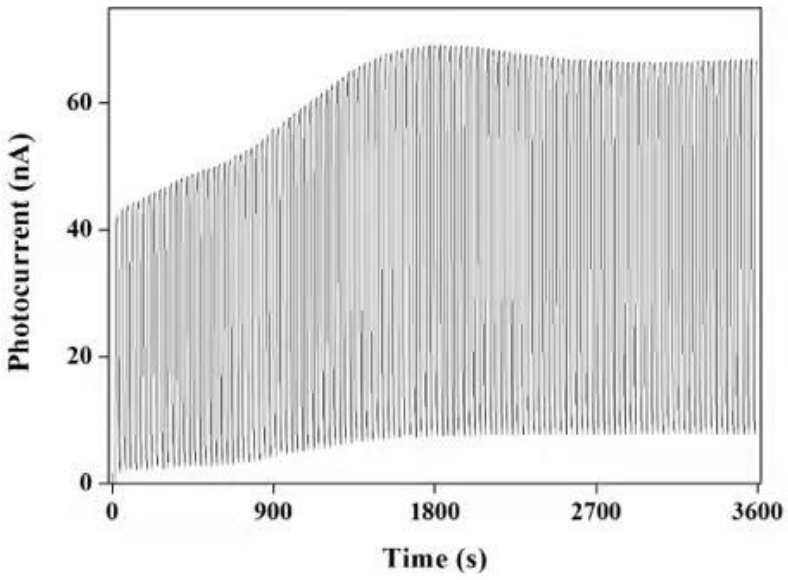

Fig. S3. The real-time monitoring of photoelectric response the coexistence system of MB and MB/high-order DNA scaffolds complex.

Results and discussion

Optimization of experimental conditions

To improve the operation performance of the as-proposed split-type PEC assay, the experimental conditions should be carefully optimized. First, both the padlock probe was hybridized with miR-21 and the resulting DNA-RNA duplex triggers the RCA polymerization was performed in homogeneous solution. The RCA reaction conditions including the amount of phi29 DNA polymerase, and the reaction time of RCA (**Fig. S4**) were optimized. The value of photocurrent change (ΔI=I-I_0) was adopted to appraise the performance of the PEC sensor, where I and I_0 were photocurrents signal responses of this PEC sensor in the presence and absence of the target miR-21, respectively. As indicated in **Fig. S4A**, the photocurrent change (ΔI) increased with the increasing amount of phi29 DNA polymerase, and then increased to a maximum value at 4 U, indicating a saturated amplification. For the polymerization time of RCA (**Fig. S4B)**, from 0.5 h to 5 h, the photocurrent change (ΔI) increases rapidly with the increase of polymerization time and reaches a plateau at 2 h. Therefore, the optimized phi29 DNA polymerase dosages of 4 U and the optimized polymerization time of 2 h were employed in the following experiments. Additionally, the amount of three short stable strands (biton-P1, P2, P3) plays an important role in formation of high-order DNA scaffolds. As shown in **Fig. S4C**, the concentration of 4 μM biton-P1, P2, P3 was found to give the best PEC response, indicating that it was sufficient for forming well-defined DNA scaffolds. Finally, in order to full removal of the target miR-21-triggered MB/DNA scaffold complex from the free MB solution, the amount of streptavidin magnetic nanobeads (strep-MB) was carefully optimized. As indicated in **Fig. S4D,** the photocurrent change (ΔI) increased with the increasing amount of strep-MB, and then increased to a maximum value at 30 μL, indicating a saturated probe load and being selected.

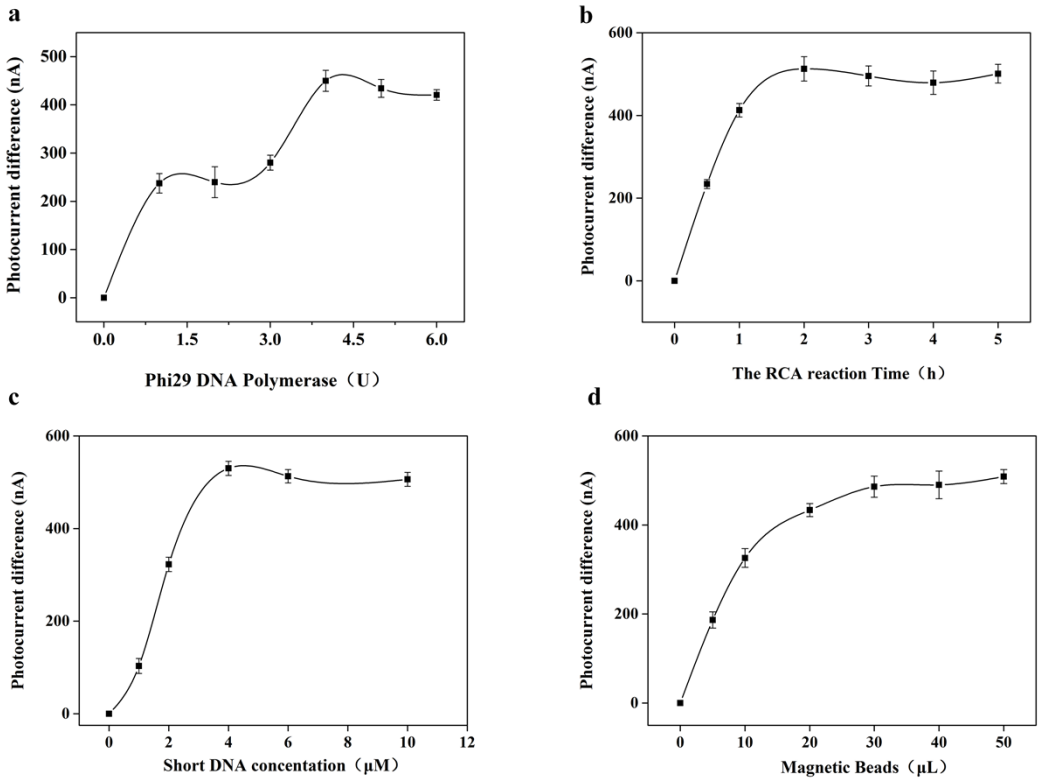

Fig. S4. Effect of the concentration of phi29 DNA polymerase (a), RCA time (b); the concentration of short DNA (c); and the concentration of magnetic beads (d) on the PEC response of sensing system.

Table S2. Comparison of different methods for miR-21 detection

method	Linear range	Detection limit (fM)	ref
Electrochemistry	10 fM - 5 nM	2.36	1
Electrochemistry	10 fM - 1.0 nM	10	2
Electrochemistry	2 fM - 1 nM	2	3
ECL	1pM - 10 nM	300	4
ECL	2.34 fM -100 pM	0.721	5
Fluorescence	0.01 nM - 200 nM	10^4	6
Fluorescence	0.2 nM - 20 nM	$9.8*10^4$	7
Fluorescence	100 fM - 50 pM	67.3	8
SERS	1.0 fM - 10 nM	0.34	9
SERS	10 fM - 100 nM	2.88	10
Photoelectrochemistry	1 fM - 1 nM	0.37	11
Photoelectrochemistry	10 fM - 1 μM	3.25	12
Photoelectrochemistry	1 pM - 100 nM	310	13
Photoelectrochemistry	10 fM - 100 nM	3.4	14
Photoelectrochemistry	**10 fM - 1 μM**	**2.443**	In this work

References

[1] P. Fu, S. Xing, M. Xu, Y. Zhao, C. Zhao, Peptide nucleic acid-based electrochemical biosensor for simultaneous detection of multiple microRNAs from cancer cells with catalytic hairpin assembly amplification. Sens. Actuators B Chem. 305 (2020) 12754-12763.

[2] D. Zeng, J. Shen, X. Mi, DNA Tetrahedral nanostructure-based electrochemical miRNA biosensor for simultaneous detection of multiple miRNAs in pancreatic carcinoma. ACS Appl. Mater. Interfaces. 9 (2017) 24118-24125.

[3] C. Fang, K. Kim, B. Yu, S. Jon, M. Kim, H. Yang, Ultrasensitive electrochemical detection of miRNA-21 using a zinc finger protein specific to DNA-RNA hybrids. Anal. Chem. 89 (2017) 2024-2031.

[4] W. Bai, A. Cui, M. Liu, X. Qiao, Y. Li, T. Wang, Signal-off electrogenerated chemiluminescence biosensing platform based on the quenching effect between ferrocene and $Ru(bpy)_3^{2+}$-functionalized meta-organic frameworks for the detection of methylated RNA. Anal. Chem. 91 (2019) 11840-11847.

[5] L. Gálvez, T. Mendiola, C. Sánchez, Carbon nanodot-based electrogenerated chemiluminescence biosensor for miRNA-21 detection. Microchim Acta. 188 (2021) 398-410.

[6] C. Wang, H. Zhang, D. Zeng, W Sun, H. Zhang, X. Zuo, X. Mi, Elaborately designed diblock nanoprobes for simultaneous multicolor detection of microRNAs. Nanoscale. 7 (2015) 15822-15829.

[7] S. Li, K. He, R. Liao, C. Chen, X. Chen, C. Cai, An interference-free and label-free sandwich-type magnetic silicon microsphere -rGO-based probe for fluorescence detection of microRNA. Talanta. 174 (2017) 679-683.

[8] X. Tang, R. Deng, Y. Sun, X. Ren, M. Zhou, J. Li, Amplified tandem spinach-based aptamer transcription enables low background miRNA detection. Anal. Chem. 90 (2018) 10001-10008.

[9] S. Wen, Y. Su, C. Dai, J. Jia, G. Fan, L. Jiang, R. Song, J Zhu, Plasmon coupling-enhanced raman sensing platform integrated with exonuclease - assisted target recycling amplification for ultrasensitive and selective detection of microRNA-21. Anal. Chem. 91 (2019) 12298-12306.

[10] X. Du, S. Wu, X. Huang, J. Sun, Ag Nanocubes coupled with heating-enhanced DSN-assisted cycling amplification for surface-enhanced raman spectroscopy detection of microRNA-21. ACS Appl. Nano Mater. 4 (2021) 2565-2574.

[11] N. Fu, L. Wang, X. Zou, C. Li, S. Zhang, B. Zhao, Y. Gao L. Wang, A photoelectrochemical sensor based on a reliable basic photoactive matrix possessing good analytical performance for miRNA-21 detection. Analyst. 145 (2020) 73888-7396.

[12] Y. Wen, M. Qing, S. Chen, H. Luo, N. Li, Y-type DNA structure stabilized p-type CuS quantum dots to quench photocurrent of ternary heterostructure for sensitive photoelectrochemical detection of miRNA. Sens. Actuators B Chem. 329 (2021) 129257.

[13] Y. Chu, R. Wu, G. Fan, A. Deng, J. Zhu, Enzyme-free photoelectrochemical biosensor based on the co-sensitization effect coupled with dual cascade toehold-mediated strand displacement amplification for the sensitive detection of microRNA-21. ACS Sustainable Chem. Eng. 6 (2018) 11633-11641.

[14] C. Huang, Y. Liu, Y. Sun, F. Wang, S. Ge, J. Yu, Cathode-anode spatial division photoelectrochemical platform based on a one-step DNA walker for monitoring of miRNA-21. ACS Appl. Mater. Interfaces. 13 (2021) 35389 - 35396.